ILASS 2008
Sep. 8-10, 2008, Como Lake, Italy

Paper ID ILASS08-2-5

NUMERICALNUMERICAL AND PHYSICAL BASIS OF AN EULERIAN MULTI-PHASE FLOW MODEL FOR THE SIMULATION OF THE LIQUID FUEL INJECTION IN INTERNAL COMBUSTION ENGINES

Francis BAYORO*, Chawki HABCHI*, Eric DANIEL°

*IFP, 1&4 avenue de Bois Préau 92852 Rueil-Malmaison Cedex, France
°Université Aix Marseille, UMR CNRS 6595 IUSTI, 5 rue Enrico Fermi 13453 Marseille cedex 13, France

ABSTRACT

The objective of this work is to develop an Eulerian multi-phase flow model in order to improve the prediction of fuel injection simulations in internal combustion Diesel engines. Lagrangian models, usually used in engines simulations, are based on the assumption of dispersed two-phase flow with low liquid volume fraction, which is not fulfilled in the case of direct injection, particularly in the dense liquid zone close to the nozzle. Moreover, because the liquid flow is compressible, cavitation phenomena may occur inside the injector leading to a highly transient injection process particularly for the fuel flow rate (discharge coefficient), spray cone angle and liquid atomization.

Different Eulerian approaches are available in the literature. Physical phenomena that occur inside and near the nozzle exit have led to the choice of a three-fluid-three-pressure model. The perfect gas equation of state (EOS) is used for the gas phase in the combustion chamber while the thermodynamics of the fuel phases (liquid or vapor) is governed by the 'Stiffened Gas' EOS. The Eulerian multi-phase flows model is currently in development in a RANS (Reynolds Averaged Navier Stokes) approach within the IFP-CFD-TPF code, a multidimensional Navier-Stokes equations solver. Several open terms appear in the equations of the model such as the mass, momentum, energy and turbulent exchanges between the two or three phases.

In this paper, only the two-phases (liquid-gas) part of the model is presented. It has been integrated using a Arbitrary Lagrangian Eulerian (ALE) formulation. On the one hand, velocities, pressures and temperatures in each phase are solved using a modified 'SIMPLE' method (Semi-Implicit Method for Pressure Linked Equations). On the other hand, convective terms are computed using a sub-cycled explicit numerical scheme.

Several validation test cases have been carried out to assess the numerical implementation and physical fundamental behavior of the two-phase model. It is shown that it is able to compute the fuel expansion in conditions similar to those of Diesel injection.

INTRODUCTION

Considering future environmental and economical requirements, motorist engineers have to develop less consuming and cleaner engines. One of the solutions adapted to these requirements is to improve combustion by acting on spray atomization. A way is to raise the liquid velocity at the nozzle exit, by increasing injection pressure and decreasing the orifice diameter. For instance, the common-rail injection system can achieve high injection pressures up to 2000 bars even at low load and speed. The dimensions of the orifice diameters have decreased nowadays to roughly 130 µm. Consequently, liquid jet velocities at full injection grow to several hundreds meters per second. These conditions make experimental analysis of the flow in the injector and near the nozzle exit very difficult. Therefore, linking the liquid jet atomization features to the internal flow characteristics in the nozzle is quite complicated. Nevertheless, available previous literature studies [1][2] have shown that several factors are to affect atomization. The challenge is now to identify each of them, and to characterize their influence on the spray in order to improve the mixture preparation and combustion modeling of high-pressure Diesel engines.

Many previous experimental [3][4][5][6] and numerical [7][8] studies have highlighted the complexity of the flow inside Diesel injectors. This flow complexity induces a sudden and strong decrease of the pressure (generally in regions near the inlet of the orifices) that leads to the appearance of the cavitation as soon as the pressure decreases below the saturation pressure of the most volatile component of the fuel. Cavitation is thus due primarily to the complex structure of the flow in the injector. Its appearance and disappearance accentuate this complexity, in particular in the stages of opening and closing of the needle of the injector. Another factor which affects the liquid flow and its atomization is the interaction with the gas in the combustion chamber. This interaction may be affected by the gas density and temperature, the injection velocity magnitude and direction. This last injection parameter has been shown to be closely related to the cavitating flow in the nozzle. Consequently, it is necessary to calculate the flow surging in the injector to predict the transitory behavior of the liquid jet and its atomization in the combustion chamber.

This study belongs to a project which aims to develop a new numerical code able to calculate at the same time the cavitating flow in the injector and the atomization of the jet in the combustion chamber. The purpose of this paper is to present the Eulerian two-phase flows model implemented using a splitting semi-implicit numerical scheme. In this work, viscous and source exchange terms have been neglected. The model solves three dimensional compressible two-phase flow. Each pure fluid (here liquid and gas) is considered as single-phased with its own pressure and velocity. The resolution of the Lagrangian part of the equations is based on the SIMPLE (Semi Implicit Method for Pressure Linked Equations) method. Next, a Quasi-Second Order Upwind (QSOU) scheme is used for convection.

This paper is organized as follows. First, we present the system of equations and its closure. Two Equations of state (EOS) for each pure fluid with 'Stiffened gas' approximations has been adopted. Next, an original numerical scheme has

been proposed to solve the system. Then a shock tube test case has been carried out in conditions *(P_L=2000 bars and P_G=50 bars*) similar to those one may obtain inside Diesel injector just after the needle opening. Finally comparisons have been done between IFP-C3D-TPF code numerical results and Riemann analytical solutions.

PRESENTATION OF IFP-C3D-TPF CODE

Equations of the model

To obtain the multiphase flows model we use the averaging method of Drew & Passman [9] applied to compressible Navier-Stokes equations of the various constituents. We neglect all dissipative terms, viscous and mass transfer terms. This model was developed in Saurel & Abgrall [10][11][12] and in Saurel & Lemetayer [13] for a two-phase system. It is inspired by the work of Baer & Nunziato [14] where a two-phase model is proposed to study the deflagration-to-detonation transition in solid energetic materials. We write here the system for two-phase flows (liquid and gas). For two-phase flows, the model consists of the seven following equations:
Two continuities equations :

$$\begin{aligned} &\frac{\partial \alpha_L \rho_L}{\partial t} + \nabla\left(\alpha_L \rho_L V_L\right) = 0 \\ &\frac{\partial \alpha_G \rho_G}{\partial t} + \nabla\left(\alpha_G \rho_G V_G\right) = 0 \end{aligned} \tag{1.1}$$

Two momentum equations :

$$\begin{aligned} &\frac{\partial \alpha_L \rho_L V_L}{\partial t} + \nabla\left(\alpha_L \rho_L V_L \otimes V_L\right) = -\nabla\left(\alpha_L P_L\right) + P_I \nabla \alpha_L \\ &\frac{\partial \alpha_G \rho_G V_G}{\partial t} + \nabla\left(\alpha_G \rho_G V_G \otimes V_G\right) = -\nabla\left(\alpha_G P_G\right) + P_I \nabla \alpha_G \end{aligned} \tag{1.2}$$

Two equations of internal energy :

$$\begin{aligned} &\frac{\partial \alpha_L \rho_L e_L}{\partial t} + \nabla\left(\alpha_L \rho_L e_L V_L\right) = -P_L \nabla\left(\alpha_L V_L\right) + P_I V_I \nabla \alpha_L \\ &\frac{\partial \alpha_G \rho_G e_G}{\partial t} + \nabla\left(\alpha_G \rho_G e_G V_G\right) = -P_G \nabla\left(\alpha_G V_G\right) + P_I V_I \nabla \alpha_G \end{aligned} \tag{1.3}$$

And then the liquid volume fraction equation to close the system:

$$\frac{\partial \alpha_L}{\partial t} + V_I \nabla \alpha_L = 0 \tag{1.4}$$

The notation is conventional. The subscripts L and G represent respectively liquid and gas phases. The volume fraction α_K is defined by the volume occupied by phase K over the total volume. The saturation constraint imposes $\sum \alpha_K = 1$. The density, velocity, pressure and internal energy for each pure fluid are denoted respectively ρ_K, V_K, P_K and e_K. We have three non-conservative terms: $V_I \nabla \alpha_K$, $P_I \nabla \alpha_K$, $P_I V_I . \nabla \alpha_K$, where P_I and V_I are respectively interfacial pressure and velocity. The knowledge of these last terms is necessary to close the system.

Equations of state

The two-phase flow is considered as non-homogeneous mixture of compressible fluid so an equation of state is necessary for each phase to close entirely the system. For the liquid phase, the following 'Stiffened Gas' (referred to below as SG) EOS is used :

$$P_L = \rho_L \left(\gamma_L - 1\right)\left(e_L - q_L\right) - \gamma_L P_{\infty,L} \tag{1.5}$$

For the gas phase, one may recover the following perfect gas EOS:

$$P_G = \rho_G \left(\gamma_G - 1\right) e_G \tag{1.6}$$

Table 1 resumes the values of the equations of state parameters (γ_K , q_K , $P_{\infty,K}$) of each phase :

Parameters	Gas	Liquid (dodecane)
γ_K	1.4	2.35
q_K	0.0 J/kg	-755269 J/kg
$P_{\infty,K}$	0.0 Pa	4.10^8 Pa

Table 1: Parameters of the Stiffened gas equations of state.

Interfacial pressure and velocity

When dealing with two-phase gas-liquid flows at low pressure and velocity, the most natural idea is to consider the liquid phase incompressible. Then, the interfacial pressure P_I is taken equal to the gas pressure. This choice yields an ill-posed mathematical model, which results in numerical instabilities during numerical resolution, or in the necessity of using an extremely large numerical viscosity yielding unrealistic solutions (see for example Drew & Passman [9]).
Other authors (Toro [15]; Sainsaulieu [16]) have proposed to introduce a pressure non-equilibrium effect, $P_I(\alpha)$. For Sainsaulieu, P_I is a perturbation term that enables the system to be hyperbolic. For Toro, this pressure represents compaction effects in a packed powder bed. Other authors (Butler et al. [17]) assume $P_I = 0$. This choice is not realistic.
In our approach, each phase is considered compressible with its own pressure and velocity. This guaranties hyperbolicity of the system. So, there is some flexibility in the choice of closure relations for interfacial pressure and velocity with respect to hyperbolicity. But for physical reasons, the interfacial pressure and velocity must be estimated as accurately as possible. Unfortunately, this is nearly impossible in the general case. For the specific context of stratified two-phase flows, it is possible to estimate an

interfacial pressure on the basis of the velocity and density differences (Bestion [18]). For flow of gases and solid particles under weak solid compressibility, it is reasonable to assume the interfacial pressure to be the gas one, and interfacial velocity to be the solid one (Baer & Nunziato [14]). In fact, for each physical situation, there are choices better than other, but none of them is perfectly satisfactory. Following Baer & Nunziato and assuming that the liquid phase is less compressible than the gas one, we used:

$$P_I = P_G$$

$$V_I = V_L$$

Because each phase is compressible, a choice preserving the symmetry of equation system may also be used as well.

Mesh and control volumes

The three dimensional mesh is made up of arbitrary hexahedron cells. The eight corners of each regular cell are the vertices. Spatial difference approximations are constructed by the control-volume or integral-balance approach, which largely preserves the local conservation properties of the differential equations. The IFP-C3D-TPF code uses a staggered grid. On the one hand, scalar variables are defined at the center of the cells. On the other hand, velocity is defined at the nodes around whose a control volume is built. This control volume is usually called momentum cell as its main use is in differencing the momentum equations. Then, momentum cells are centered on the vertices. Figure 1 shows a two dimensional momentum cell for instance.

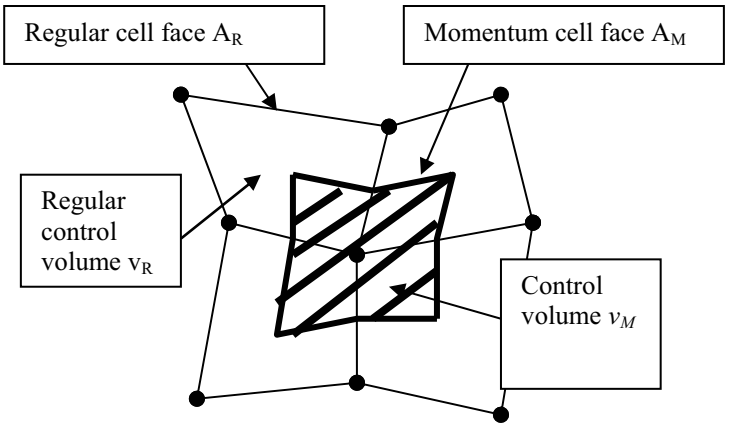

Figure 1 : Momentum and regular control volumes in a two dimensional mesh case.

In contrast to the regular cells, which have six faces, momentum cells have twenty-four faces if the mesh is structured. Each of which is comparable in size to one-fourth of a regular cell face. In the case of unstructured mesh as in IFP-C3D-TPF code, the number of momentum cell faces is unknown a priori. Three of these momentum cells faces lie in each of the regular cells. The points of intersection of the momentum cell faces with the regular cell edges are defined as the midpoints of the regular cell edges. The points of intersection of the momentum cell edges with the regular cell faces are subsquently defined implicitly by the requirement that the regular cell face be partitioned into four sub-faces of equal area by the momentum cell faces. The corners of the momentum cells are subsquently implicitly defined by the requirement that the overlap volume between a regular cell and a momentum cell centered at one of its corners be one-eighth of the regular cell volume. In general, the momentum cell corners do not coincide with the cell centers. The momentum cell corners and the intersection points of momentum cell edges with regular cell faces are not actually solved for as they are not needed.
The location of velocities at cell vertices is convenient because no interpolation is required when determining vertex motion in the Lagrangian phase of the calculation.

Numerical Scheme and system resolution

We adopt the finite-volume method to solve the system. Assuming the physical variables $\phi_K = \alpha_K$, $\alpha_K \rho_K$, $\alpha_K \rho_K V_K$, $\alpha_K \rho_K e_K$ to be known at step time n, we solve the system to get ϕ_K at time n+1.

Two phases (denoted B and C) are considered to get ϕ_K^{n+1} values.
In the phase B , we solve pressure terms in the momentum and internal energy equations:

$$\frac{\partial \alpha_K \rho_K V_K}{\partial t} = -\nabla(\alpha_K P_K) + P_I \nabla \alpha_K \tag{1.7}$$

$$\frac{\partial \alpha_K \rho_K e_K}{\partial t} = -P_K \nabla(\alpha_K V_K) + P_I V_I \nabla \alpha_K \tag{1.8}$$

After integration (1.7) on the momentum cell v_M and the (1.8) on the regular cell v_R defined in Figure 1 , one can obtain:

$$V_K^B = V_K^n - \frac{\Delta t}{M_{K,M}^B}\left(\sum_{S_M}\left(\left[\alpha_K^n P_K^B\right]_{S_M} - P_{I,M}^B\left[\alpha_K^n\right]_{S_M}\right)A_M^n\right) \tag{1.9}$$

$$e_K^B = e_K^n - \frac{\Delta t}{M_{K,R}^B}\left(\sum_{S_R} P_K^B\left(\left[\alpha_K^n V_K^B\right]_{S_R} - P_I^B V_{I,R}^B\left[\alpha_K^n\right]_{S_R}\right)A_R^n\right) \tag{1.10}$$

Where $M_{K,M}^B = (\alpha_K \rho_K v_M)^B$ is the phase K mass at time B in the momentum control volume v_M. A_M^n represents the momentum cell area and $[Q_K]_{S_M}$ is the value the physical variable Q in the phase K on the face S_M.
$M_{K,R}^B = (\alpha_K \rho_K v_R)^B$ is the phase K mass at time B in the regular control volume v_R. A_R^n represents the area of regular cell . $P_{I,M}^B$ is the value of interfacial pressure at the center of momentum cell and $V_{I,R}^B$ is the value of the interfacial velocity at the center of the regular cell. Their expressions are given below:

$$P^B_{I,M} = \frac{\sum_{j=1}^{N} \alpha^A_{I,j} P^B_{I,j}}{\sum_{j=1}^{N} \alpha^A_{I,j}}$$
$$V^B_{I,R} = \frac{\sum_{i=1}^{8} \alpha^A_{I,i} V^B_{I,i}}{\sum_{i=1}^{8} \alpha^A_{I,i}} \quad (1.11)$$

where the subscript *I* represents the eight nodes of the regular control volume and N is the number of regular cells linked to the momentum control volume v_M.

In the phase C, we solve the convective terms:

$$\frac{\partial \phi_K}{\partial t} = -\nabla.\left(\phi_K V_K\right) \quad (1.12)$$

The integration on the control volume gives:

$$\phi_K^{n+1} v_{K,R}^{n+1} = \phi_K^B v_{K,R}^B + \sum_{S_R}^{6} \left[\phi_K^B\right]_{S_R} \left[\delta v_K^B\right]_{S_R} \quad (1.13)$$

Where $\left[\delta v_K^B\right]_{S_R} = \left[VA_R\right]^B_{K,S_R} \Delta t$ represents the volume swept by the face *S* of the regular control volume during the Lagrangian phase B. Then, the pressures are determined by the equations of state:

$$P_K^{n+1} = EOS\left(\rho_K^{n+1}, e_K^{n+1}\right) \quad (1.14)$$

Calculation of the flow rate $\left[VA_R\right]^B_K$ is the originality of the particular SIMPLE method used in phase B of IFP-C3D-TPF code. We solve the following complementary equation:

$$\frac{D}{Dt}\int_{v_f}\left[\alpha_K \rho_K V_K A_R\right]dv = \int_{v_f} F.A_R dv + \frac{DA_R}{Dt}\int_{v_f}\left[\alpha_K \rho_K V_K\right]dv \quad (1.15)$$

where v_f is a control volume about a face A_S of the regular cell (see Figure 2) and the expression of *F* is given by $F = -\nabla\left(\alpha_K P_K\right) + P_I \nabla \alpha_K$

The integration of this equation yields to the following numerical scheme:

$$\left[VA_R\right]^B_K = \left[VA_R\right]^n_K + \left[\frac{DA_R}{Dt}\right]^n . V^n_{K,f} + F^* \quad (1.16)$$

where the expression of F^* is given by:

$$F^* = -\frac{\Delta t}{M^B_{K,f}}\left[\sum_f \left(\alpha^n_K P^B_K\right)_f A^n_f A^n_R - P^B_{I,f} \sum_f \alpha^n_K A^n_f A^n_R\right]$$

and :

$$\left[\frac{DA_R}{Dt}\right]^n = \frac{A^t_R - A^n_R}{2\Delta t}$$
$$V^n_{K,f} = \frac{1}{4}\sum_{i=1}^{4} V^n_{K,i} \quad (1.17)$$
$$\left[VA_R\right]^n_K = \frac{A^n_R}{4}\sum_{i=1}^{4} V^n_{K,i}$$

Where $M^B_{K,f} = \left(\alpha_K \rho_K v_f\right)^B$ is the phase K mass at time B in the control volume v_f. A^t_R represents the area of the face A_R after its four corners displacement. Its expression is given as follow:

$A^t_R = A_R\left(x_n + V^n_K \Delta t\right)$. x_n is the face A_R corner position at the step time n.

$P^B_{I,f}$ is the value of the interfacial pressure in the control volume v_f given by:

$$P^B_{I,f} = \frac{\alpha^n_{I,l} P^B_{I,l} + \alpha^n_{I,r} P^B_{I,r}}{\alpha^n_{I,l} + \alpha^n_{I,r}}$$

where the subscripts *l* and *r* designate the cells around the face A_R. The subscript I designates interfacial parameters value.

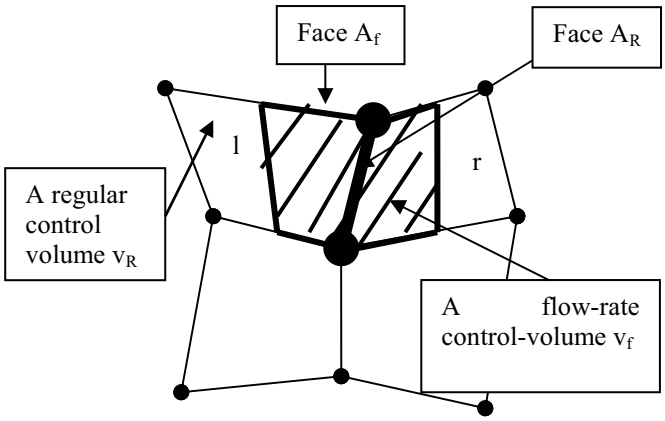

Figure 2 : Control volume v_f for the computation of the flow rate $\left[VA_R\right]^B_{K,f}$.

The knowledge of the flow rate $\left[VA_R\right]^B_K$ allows to determine the volume v^B_K occupied by the phase K at the end of the Lagrangian phase B as we have:

$$v^B_K = v^n_K + \Delta t \sum_{S_R=1}^{6} \left[VA_R\right]^B_{K,S_R} \quad (1.18)$$

In the expression above, the summation is done on the six faces of the regular cell or scalars control volume.

This volume must be compared to the volume $v^B_{K,EOS}$, given by the equation of state:

$$v^B_{K,EOS} = \frac{(\gamma_K - 1) C_{V,K} T^B_K}{P^B_K + P_{\infty,K}} \tag{1.19}$$

where T^B_K is the phase K temperature. Using the equation of internal energy (Eq 1.9) and the following equation of state:

$$e^B_K = \frac{P^B_K + \gamma_K P_\infty}{P^B_K + P_{\infty,K}} C_{V,K} T^B_K + q_K \tag{1.20}$$

one can obtain:

$$T^B_K = \frac{e^n_K + \frac{\Delta t}{M^B_{K,c}} E^*}{\frac{P^B_K + \gamma_K P_{\infty,K}}{P^B_K + \gamma P_{\infty,K}} C_{V,K}} \tag{1.21}$$

where E^* is given by:

$$E^* = -P^B_K \sum_{S_R}^{6} \left[\alpha^n_K V^B_K\right]_{S_R} A^n_{S_R} + P^B_I V^B_{I,R} \sum_{S_R}^{6} \left[\alpha^n_K\right] A^n_{S_R} \tag{1.22}$$

To account for the compressibility of the two phases, the isentropic form of the equation of state is used to correct the volume $v^B_{K,EOS}$.
In the first iteration of the SIMPLE method, an estimated of the pressure $P^{B^*}_K$ is :

$$P^{B^*}_K = P^{B_{n-1}}_K + \frac{\Delta t^n}{\Delta t^{n-1}} \left[P^{B_{n-1}}_K - P^{B_{n-2}}_K \right] \tag{1.23}$$

where $P^{B_{n-2}}_K$ and $P^{B_{n-1}}_K$ stand respectively for pressure values at the times (n-2) and (n-1). This initial pressure is used to get the corrected form of the volume $v^B_{K,EOS}$ (Eq 1.19) as follow:

$$v^{B,C}_{K,EOS} = v^B_{K,EOS} \left[1 + \frac{1}{\gamma_K + \frac{P_{\infty,K}}{P^B_K}} \left(1 - \frac{P^B_K}{P^n_K} \right) \right] \tag{1.24}$$

This volume $v^{B,C}_{K,EOS}$ is compared to the volume v^B_K (given by (1.18)) swept by the faces of the regular cell by calculating the residual *res* between these two terms.

$$res = v^{B,C}_{K,EOS} - v^n_K - \Delta t \sum_{S_R}^{6} \left[VA_R\right]^B_{K,S_R} \tag{1.25}$$

The numerical scheme for advection consists in a Quasi-Second Order Upwind scheme (QSOU) as reported in Amsden et al. [19], which ensures the monotonicity of the solution. In other words no negative values (by oscillations) may be obtained, despite pressure and density ratios are tremendous. This is very important with regards to calculation robustness.

As we use an explicit scheme, in phase C, the time step has to obey the following stability criterion:

$$Max\left(\frac{\left[VA\right]_{S_R} \Delta t}{v_R} \right) \leq 1 \tag{1.26}$$

The modified SIMPLE iterative algorithm

We resume the SIMPLE algorithm as follows:

(1) Evaluation of guessed pressures $P^{B^*}_K$ Eq. (1.23);

(2) Update the pressure fields P^B_K using Eq. (1.24) and calculate the flow rate $\left[VA_R\right]^B_K$;

(3) Update the temperature fields T^B_K : (Eq. 1.20);

(4) If the pressure field is non converged, $P^{B^*}_K = P^B_K$ and go back to step (2).

At convergence, the velocity field V^B_K and the internal energy e^B_K are updated using (Eq (1.9)) and (Eq (1.10)) respectively.

Validation of the model

In order to validate the two-phase flow model and to check the numerical scheme accuracy, we carried out several tests. We present in this paper a shock tube test-case (see Figure 3). It is a tube with an interface between two pure fluids. A pure liquid (here dodecane) has been settled in the left side under high pressure (2000 bars) and a gas in the right side under low pressure (50 bars). This conditions are the one that can be observed in the recent injectors during the injector opening. Temperature in the domain is set to 300 K. The basic solution of this problem is well-known. Simulation has been done up to the time 200 µs using the model implemented in Fortran 90 within the IFP-C3D-TPF code.

The numerical results have been compared to the analytical ones given by a Riemann solver (Figure 4 to Figure 8). One can observe the perfect coincidence between the two results except a little difference between axial velocity solutions which can be seen in Figure 6 near the interface in the gas side. This difference could be explained by the numerical diffusion due to non-conservative terms ($P_I \nabla \alpha_K$, $P_I V_I . \nabla \alpha_K$) discretization. Indeed, for numerical reason, a small amount of liquid ($\alpha_L = 0.001$) has been initialized in the part of gas domain so that a little variations of liquid in the right side of the interface (in the gas) could induce high effects.

The positions of the interface liquid-gas at the initial time and at 200 µs (Figure 4) show that the two-phase flow propgates to the right side of the tube. An expansion wave can be seen in the liquid and a choc wave appears in the gas. Figure 6 shows that the maximum velocity reached by the flow is of about 150 m/s.

The appearance of an expansion wave on the liquid side can be confirmed on Figure 7 and Figure 8: at 200 µs, the liquid temperature and density have decreased considerably, whereas the gas temperature and density have increased due to the compression wave.

These results indicate that the model presented in this paper is able to simulate the flow induced by the injection pressure during the opening of Diesel injector for instance.

Liquid: Dodecane P_L = 2000 bars α_L = 0.999 T_L = 300K	Gas: Air P_G = 50 bars α_G = 0.999 T_G = 300K

Figure 3 : Liquid and Gas in a shock tube

CONCLUSIONS

In this paper we presented a 3D inviscid two-phase flows model in order to simulate liquid/gas flows both in Diesel injectors and in the combustion chamber. An original numerical scheme based on the SIMPLE method has been proposed in order to solve the Eulerian two-phase two-pressure model. Numerical solutions have been compared to the analytical ones to validate the numerical model. A perfect agreement have been observed between the numerical results and the analytical solutions of a shock-tube test case.

In future work the model proposed will be used with the same numerical scheme to treat a cavitation problem in order to study its influence on spray atomization.

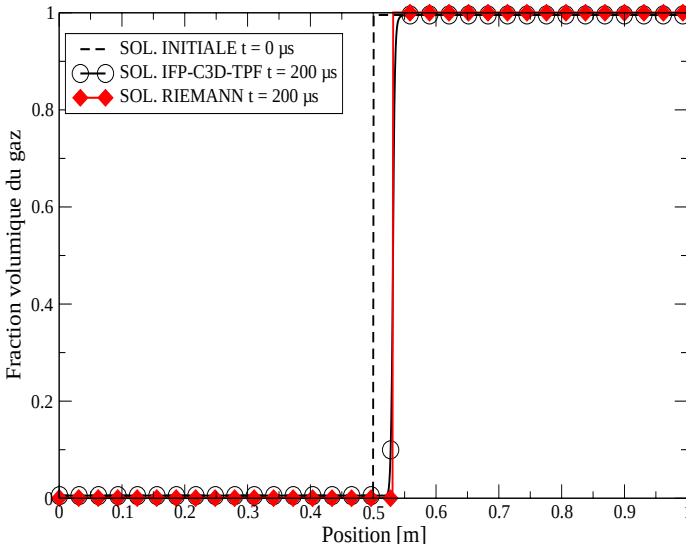

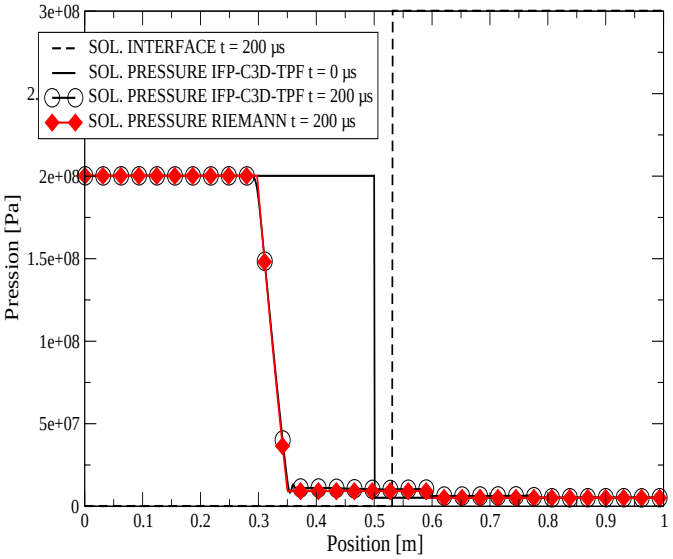

Figure 5 : Pressure field in the tube

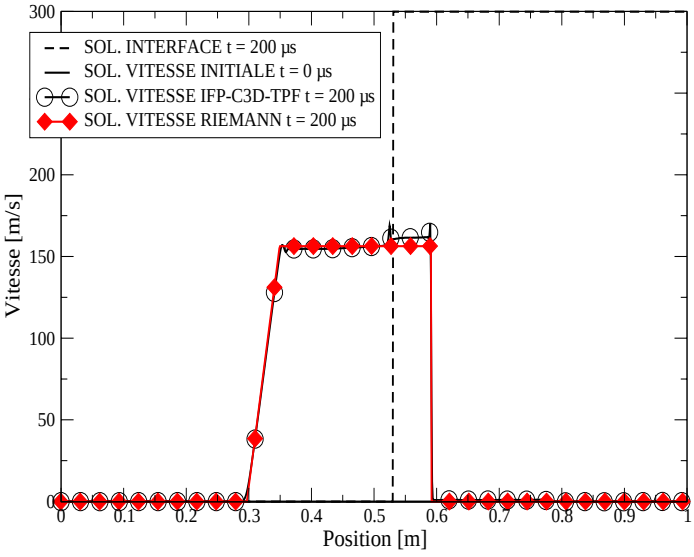

Figure 6 : Velocity field in the tube

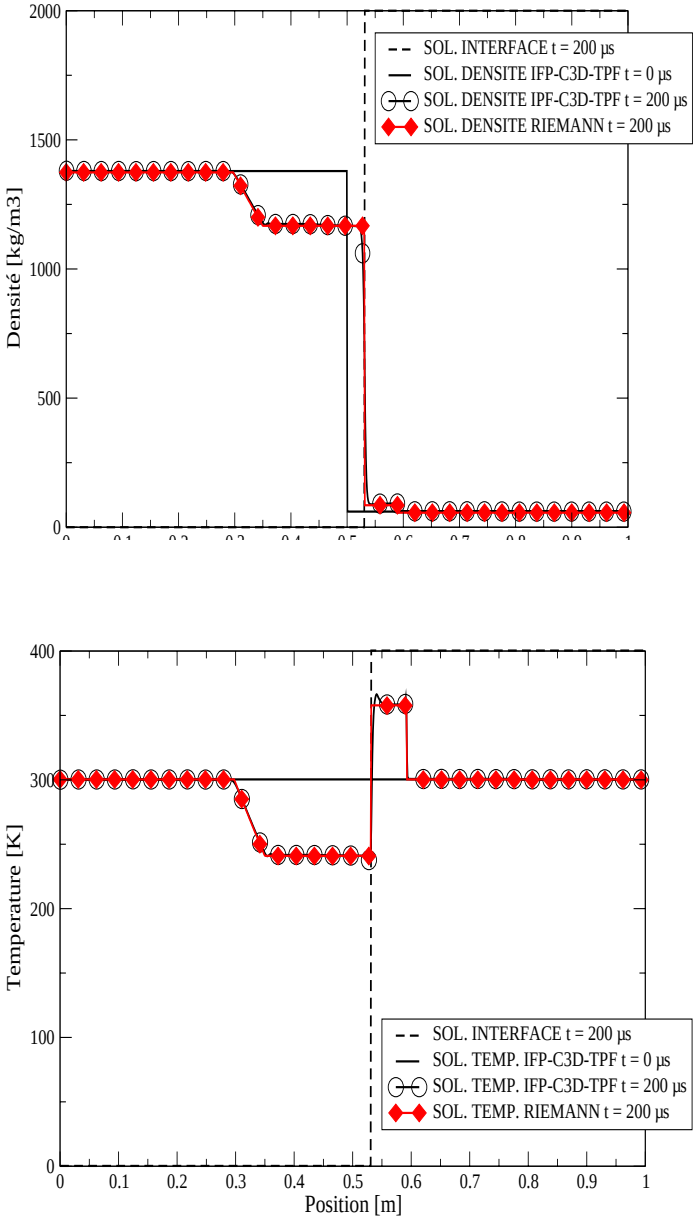

Figure 8 : Fluid temperature in the tube

REFERENCES

[1] Tamaki, N., Shimizu, M., Nishida K. & Hiroyasu H., Effects of Cavitation and Internal Flow on Atomization of a liquid jet. Atomization and Sprays, vol. 8, pp. 179-197, 1998.

[2] Dumont, N., Simonin, O. & Habchi, C., Cavitating Flow in Diesel Injectors: A Bibliographical Review, 18th ICLASS Proceedings, Pasadena, CA, USA, pp. 314-323, 2000.

[3] Arcoumanis, C., Badami, M., Flora, H., & Gavaises, M., Cavitation in real-size Multi-Hole Diesel Injector Nozzle, SAE paper N° 1999-01-1249, 2000.

[4] Soteriou, C., Andrews, R., Torres, N., Smith, M. & Kunkulagunta, R., Through the Diesel Nozzle Hole – A journey of Discovery, 14th ILASS America Proceedings, Dearborn, MI, USA, pp. 78-85, paper 17, 2001.

[5] Blessing, M., Konig, C., Kruger, C., Michels, U. & Schwartz, V., Analysis of Flow and Cavitation Phenomena in Diesel Injection Nozzles and its Effects on Spray and Mixture Formation, SAE paper N° 2003-01-1358, 2003.

[6] Saliba, R., Baz, I., Champoussin J-C., Lance, M. & Marié, J-L., Cavitation Effect on the Near Nozzle Spray Development in High Pressure Diesel Injection, 19th ILASS Europe Proceedings, Nottingham, pp. 302-307, 2004.

[7] Marcer, R., Le Cottier, P.,Chaves, H., Argueyrolles, B., Habchi, C. & Barbeau B., Validated Numerical Simulation of Diesel Injector Flow Using a VOF Method, SAE Paper N° 2000-01-2932, 2000.

[8] Habchi, C., Dumont, N. & Simonin, O., Multidimensional Simulation of Cavitating Flows in Diesel Injectors by a Homogeneous Mixture Modeling Approach, Atomization and Sprays, Vol. 18, pp. 129-162, 2008.

[9] Drew, D. A. & Passman, S. L. Theory of multicomponent fluids. Springer. 1998

[10] Abgrall, R. How to prevent pressure oscillations in multicomponent flow calculations: A quasi conservative approach. J. Comput. Phys. 125, 150-160. 1996.

[11] Saurel, R. & Abgrall, R. A multiphase Godunov method for compressible multifluid and multiphase flows. J. Comput. Phys. 150, 425-467. 1999

[12] Saurel, R. & Abgrall R. A simple method for compressible multifluid flows. SIAM J. Sci. Comput. 21, 1115-1145. 1999.

[13] Saurel, R. & Lemetayer, O. A multiphase model for compressible flows with interfaces, shocks, detonation waves and cavitation. J. Fluid. Mechanics 431, 239-271. 2001.

[14] Baer, M. R. & Nunziato, J. W. A two-phase mixtuure theory for the deflagration-to-detonation transtion (DDT) in reactive granular materials. Int. J. Multiphase Flows. 12, 861-889. 1986

[15] Toro, E. F. Riemann-Problem based techniques for computing reactive two-phase flows. In Proc. Third. Intl Conf. on Numerical Combustion (ed. Dervieux & Larrouturrou). Lecture notes in Physics, vol. 351, 472-481. Antibes, France. 1989

[16] Sainsaulieu, L. Finite volume approximations of two phase fluid flows based on an approximate Roe-type Riemann solver. J. Comput. Phys. 121, 1-28. 1995.

[17] Butler, P. B. & Lambeck, M. F. & Krier, H. Modelling of shock development and transition to detonation initiated by burning in porous propellant beds. Combust. Flame 46, 75 93. 1982.

[18] Bestion, D. The physical closure laws in the CATHARE code. Nucl. Engng Design 124, 229-245. 1990.

[19] Amsden, A. & O'Rourke, P. & Butler, T. Tech. Report No. LA-11560-MS, Los Alamos Natonal Lab. 1989

Nomenclature

Symbols	***Quantity***	***SI Units***
A	Surface	m^2
C_V	Calorific capacity at constant volume	$J/kg/K$
e	Internal energy	J/kg
M	Mass	kg
P	Pressure	Pa
q	Formation energy of pure fluid	J/kg
T	Temperature	K
V	Velocity	m/s
v	Volume	m^3
	Greek Symbols	
α	Volume fraction	
$[\delta v]_{S_R}$	Volume swept by a regular control volume surface S_R	m^3
Δt	time step	s
γ	Stiffened gas EOS parameter	
ρ	Density	kg/m^3
	Subscripts	
f	Control volume v_f value	
G	Gas phase value	
I	Interface value	
L	Liquid phase value	
M	Momentum control volume value	
R	Regular control volume value	
∞	Value at infinity	
EOS	Calculation of a quantity using equations of state	
	Superscripts	
B	Variable value in the phase B of SIMPLE method	
B^*	Guessed value in SIMPLE iteration method	
B_n	Variable value obtained at the end of the phase B at the time step n	
n	Time step n	